HHS Public Access

Author manuscript

Instrum Sci Technol. Author manuscript; available in PMC 2023 May 11.

Published in final edited form as:

Instrum Sci Technol. 2017 April 27; 46(1): 102–114. doi:10.1080/10739149.2017.1311912.

Optimization of the linear quantification range of an online trypsin digestion coupled liquid chromatography–tandem mass spectrometry (LC–MS/MS) platform

Zsuzsanna Kuklenyik,

Jeffrey I. Jones,

Christopher A. Toth,

Michael S. Gardner,

James L. Pirkle,

John R. Barr

Division of Laboratory Sciences, Centers for Disease Control and Prevention, Atlanta, Georgia, USA

Abstract

Tandem mass spectrometry (MS/MS)-based proteomic workflows with a bottom-up approach require enzymatic digestion of proteins to peptide analytes, usually by trypsin. Online coupling of trypsin digestion of proteins, using an immobilized enzyme reactor (IMER), with liquid chromatography (LC) and MS/MS is becoming a frequently used approach. However, finding IMER digestion conditions that allow quantitative analysis of multiple proteins with wide range of endogenous concentration requires optimization of multiple interactive parameters: digestion buffer flow rate, injection volume, sample dilution, and surfactant type/ concentration. In this report, we present a design of experiment approach for the optimization of an integrated IMER-LC–MS/MS platform. With bovine serum albumin as a model protein, the digestion efficacy and digestion rate were monitored based on LC–MS/MS peak area count versus protein concentration regression. The optimal parameters were determined through multivariate surface response modeling and consideration of diffusion controlled immobilized enzyme kinetics. The results may provide guidance to other users for the development of quantitative IMER-LC–MS/MS methods for other proteins.

Keywords

Design of experiment; immobilized enzyme reactor; liquid chromatography–tandem mass spectrometry; proteomics; trypsin digestion

CONTACT Zsuzsanna Kuklenyik, ZKuklenyik@cdc.gov, Division of Laboratory Sciences, Centers for Disease Control and Prevention, 4770 Buford Hwy, Atlanta, GA 30341, USA.

Color versions of one or more of the figures in the article can be found online at www.tandfonline.com/list.

Supplemental data for this article can be accessed on the publisher's website.

Introduction

Quantitative analysis of proteins by liquid chromatography–tandem mass spectrometry (LC–MS/MS) relies on mass selective detection of unique protein specific peptides that are released through site-selective proteolytic cleavage, usually done by trypsin. Enzymatic cleavage and quantification based on target peptides is an attractive approach because it allows direct measurement of multiple proteins in the same sample analysis.

The typical proteomics workflow includes predigestion denaturation, alkylation, reduction, overnight digestion, and solid-phase extraction or peptide-specific antibody affinity cleanup,[1] leading to labor intensive, time consuming, and expensive workflows.[1–9] These workflows usually require the use of long digestion times to enhance digestion efficacy that increases detection of low concentration proteins and increased sequence coverage for discovery applications. However, for quantitative protein measurements, these multistep workflows present several sources of method bias and variability.

For targeted quantitative measurements, complete digestion is not a priority, if purified proteins are available as calibration standards and stable isotope labeled cleavage peptide analogs are used as internal standards. For quantitative proteomics, reproducibility and linearity in the concentration range of interest are the main priorities. A way to achieve better reproducibility is using a flow-through immobilized enzyme reactor (IMER), or “plug flow” reactor, that is online coupled with a LC–MS/MS system.[10–15] Precise control of digestion buffer flow rate and constant trypsin column void volume give integrated IMER-LC–MS/MS systems enhanced method reproducibility.[10–13] Furthermore, because of the short digestion time (typically 2–6 min) and immediate transfer for LC–MS/MS analysis, potential degradation of the peptides cleavage products and internal standard analogs are minimized without the need for sample reduction and alkylation.[10]

Theory

The reaction kinetics of flow-through trypsin IMERs differ from homogeneous, in-solution enzyme reactions because of a stagnant solvent layer between the protein carrying mobile phase and the trypsin containing stationary phase (Figure 1).[16] Inside the IMER, which usually contains porous particles, the protein molecules carried by the mobile phase have to diffuse through the stagnant liquid layer around the particles and partition into the particle pores, where the trypsin cleavage reaction takes place. After cleavage, the peptide products have to leave the enzyme active site, partition into the stagnant mobile phase layer, diffuse into the bulk mobile phase, and be carried out of the IMER.

To describe IMER reaction kinetics, certain assumption is necessary. First, the IMER is assumed to be an ideal plug-flow reactor,[16] meaning that the substrate stream flows at an even velocity with no back mixing, all protein molecules have an equal opportunity for reaction, and all products emerge and elute with the mobile phase without retention or degradation. Second, each cleavage site on the protein is an independent reaction site that releases a unique cleavage product with a unique reaction rate and digestion efficacy. Third, with large excess of immobilized trypsin inside the pores, each cleavage reaction is fast

relative to the rate of protein diffusion into the pores. With these assumptions, the diffusion of the protein substrate into the pores and the peptide products from the pores are linked in a steady-state equilibrium:

$$k_{LS} \times ([S_0] - [S]) = k_{LP} \times ([P] - [P_0]) \quad (1)$$

where k_{LS} and k_{LP} are the mass transfer coefficient of the protein substrate and peptide products, respectively. $[S_0]$ and $[P_0]$ are the concentration of the protein and peptide in the bulk mobile phase and near the diffusion boundary, while $[S]$ and $[P]$ are corresponding concentrations in the partition boundary (Figure 1.). $k_L = D_i/\delta$, where D_i is the diffusion coefficient of the protein or peptide, and δ is the thickness of the stagnant mobile phase layer. The driving force of the protein diffusion is $[S_0] - [S]$ whereas the driving force of the peptide diffusion is $[P] - [P_0]$. If $[S_0] \gg [S]$ and $[P] \gg [P_0]$, a simplified form of equation (1) can be used:

$$k_{LS} \times ([S_0]) = k_{LP} \times ([P]) \quad (2)$$

In the case of an integrated IMER-LC–MS/MS system, the peptides are recovered on a trapping column, and after the digestion, a divert valve switch allows the transfer of the cleavage products into the online coupled LC–MS/ MS system. Thus, if n_P is the mole amount of peptide produced in the IMER and Vol_{inj} is the injected sample volume, the average concentration of the product in the injection plug leaving the IMER (different from $[P_0]$ which is at the diffusion boundary) can be given by

$$[P_{out}] = \frac{n_P}{Vol_{inj}} \quad (3)$$

From $[P_{out}]$ and the protein concentration in the sample, $[S_{inj}]$, the IMER performance can be evaluated with the digestion efficacy (χ) calculated by

$$\chi = \frac{[P_{out}]}{[S_{inj}]} \quad (4)$$

The average IMER cleavage rate ($\bar{v}$) can be calculated from $[P_{out}]$ and the reaction time (t_R),

$$\bar{v} = \frac{[P_{out}]}{t_R} \quad (5)$$

By calculating t_R from the column void volume (Vol_{col}) and the volumetric flow rate of the digestion buffer (F), ($t_R = Vol_{col}/F$), and using equations (3) and (4), the average peptide cleavage rate can be also expressed as

$$\bar{v} = \chi \times \frac{F}{Vol_{col}} \times [S_{inj}] \quad (6)$$

In application for quantitative measurement of $[S_{inj}]$ in unknown samples, an LC–MS/MS peptide peak area versus $[S_{inj}]$ calibration curve needs to be constructed. The goal of the method optimization is to find a workable concentration range where the calibration curve is approximately linear whereas the signal-to-noise ratio is sufficient for reproducible and sensitive concentration measurements. For this optimization, the LC–MS/MS peak areas can be monitored to get relative estimates of $[P_{out}]$, χ and $\bar{v}$ by the following calculations:

$$[P_{out}] \sim \frac{[\text{area}]}{\text{Vol}_{inj}} \tag{7}$$

$$\chi \sim \frac{[\text{area}]}{[S_{inj}] \times \text{Vol}_{inj}} \tag{8}$$

$$\bar{v} \sim \frac{[\text{area}]}{\text{Vol}_{inj}} \times \frac{F}{\text{Vol}_{col}} \tag{9}$$

In this work, digesting bovine serum albumin (BSA) with a commercial immobilized trypsin column, we examined the empirical interrelationship among detergent concentration, $[S_{inj}]$, F, and V_{inj} using design of experiment (DoE), and multivariate correlation analysis approach.

Experimental

The materials, the IMER-LC–MS/MS instrumentation, and the DOE methodology are described in detail in the Supporting Information. The digestion buffer was 50 mM Tris and 2 mM CaCl at pH 8.4. The Trypsin column dimensions were 2.1 mm × 33 mm from Perfinity Biosciences (West Lafayette, IN, USA).

We performed four experiments with method parameters as summarized in Table 1. For each experiment, design tables were created using JMP Statistical Discovery software (SAS Institute Inc., Cary, NC, USA). We used either Invitrosol (Thermo Fisher Scientific, Waltham, MA, USA) or Zwittergent 3–12 (EMD Millipore, Billerica, MA, USA) as detergents added only to the sample.

For each monitored product ion, the absolute LC–MS/MS peak area [abs. area] was divided with the maximum peak area during each experiment of 1–4, giving normalized peak areas, [n.area]. After examination of the [n.area] versus $[S_{inj}]$ curves, four BSA peptides were selected for optimization, based on agreement between corresponding [n.area] versus $[S_{inj}]$ product ion curves. Normalized linear regression slopes were also modeled (Supporting Information), [n.area] = [n.slope] × $[S_{inj}]$ + intercept.

Results

The effect of temperature was examined separately. The minimum temperature that still gave significant improvement in all detectable peptide peak areas was 50°C (Supporting Information), which was used for all other experiments.

Based on experiments 1–4, Zwittergent 3–12 in the range of 0.05–1% concentration gave twofold higher LC–MS/MS peptide signal intensities than Invitrosol in the range of 0.05 × −2.5× (at same BSA concentration). Representative experimental peak area versus BSA concentration profiles are shown in Figure 2. At relatively high detergent and BSA concentration, Experiments 1 and 2, the profiles showed a negative curvature (Figure 2a and 2b), while at low detergent and BSA concentration, experiments 3 and 4 showed positive curvature (Figure 2c and 2d).

Response surface modeling

For finding a workable concentration range where the calibration curve is approximately linear, and for better understanding the underlying interrelationships (cross-effects) between the method parameters, we constructed multivariate least-squares fit response surface models based on experiments 1–4. We used equations (6)–(8) to estimate relative [P_{out}], χ and $\bar{v}$. The response surface prediction profiles with Zwittergent (Experiments 2 and 4) are shown in Figures 3 and 4, whereas Invitrosol (Experiments 1 and 3) are shown in the Supporting Information.

The least-squares fit models revealed several direct and cross-parameter effects. Similarly to the observed profiles in Figure 2, the [n.area] versus [S_{inj}] and [P_{out}] versus [S_{inj}] the multivariate model predicted profiles had a negative curvature above 1000 nmol/mL BSA concentrations (Figure 3) and a slightly positive curvature under 20 nmol/mL (Figure 4). The model predicted [n.area] and [P_{out}] profiles corresponded with the χ versus [S_{inj}] and $\bar{v}$ versus [S_{inj}] profiles approaching a minimum at both high and low BSA concentrations.

The model predicted χ and $\bar{v}$ increased with Zwittergent concentration, indicating enhanced IMER performance. However, above 0.1% Zwittergent [above the critical micelle concentration (CMC) of Zwittergent 3–12], the effect is diminished. At the same time, increasing Vol_{inj} had a positive effect on [n.area] only at low BSA concentration. Increasing F had a negative effect on [n.area] and [P_{out}] at low BSA concentrations but no significant effect at high BSA concentration (Figure 3 versus Figure 4).

The curvature of the model-predicted profiles was the result of significant cross effects: [S_{inj}] × F, [S_{inj}] × Vol_{inj}, F × Vol_{inj}, [detergent concentration] × Vol_{inj}, and [detergent concentration] × F cross-effects. Because of these cross effects, the LC–MS/MS signal response versus [S_{inj}] relationship is approximately linear only in a relatively narrow protein concentration range and experimental conditions. Finding this narrow range of optimal conditions for quantification can be a complex and time-consuming task by trial and error. Fortunately, the DOE approach is especially helpful for this kind of optimization problem.

Discussion

In an ideal plug-flow trypsin IMER, there is enough immobilized trypsin to keep the protein concentration at the partition boundary to be low, [S_0] ≫ [S], and removal of the products is efficient to keep peptide concentration near the diffusion boundary to be low, [P] ≫ [P_0]. With these conditions, the LC–MS/ MS response as a function of [S_{inj}] would be always linear. However, in actual application, at high protein concentration, there is not an excess

of immobilized trypsin, and the cleavage product removal is less efficient. Furthermore, concentration gradients of the protein and the peptide near the porous particle surface are influenced by both the charge and hydrophobicity of the surface, which can lead to accumulation of both the protein and the peptide at the partitioning boundary, as represented by dashed lines in Figure 1. These non-idealities exhibit themselves in positive or negative curvature as seen in the experimental data (Figure 2). Thus, in a wider concentration range, the [abs.area] versus [S_{inj}] relationship follows an S-shaped curve, with an approximate linear range in the middle. The goal of the optimization is the identification and extension of this linear range for rugged and reproducible quantitative analysis.

Effect of protein concentration in the injection solution

At low (0.05–10 nmol/mL) BSA concentrations, we observed significant positive curvature for the experimental [abs.area] versus [S_{inj}] profiles (Figure 2c and 2d). This is most likely because a minimal level of [S_0] and [P] is necessary at the partition boundary to induce peptide diffusion across the stagnant solvent layer and subsequent product elution from the IMER (driven by the ([P] − [P_0]) concentration difference). With further increase of [S_{inj}], [n.area] versus [S_{inj}] steadily increases in an approximately linear fashion. However, as the decline of χ versus [S_{inj}] and $\bar{v}$ versus [S_{inj}] shows (Figures 3 and 4), the cleavage product formation both per injected protein amount and per reaction time is gradually declining. This decline starts to occur at quite low, approximately 1 nmol/mL BSA concentration and gradually continues up to approximately 1000 nmol/mL. At very high BSA concentrations, >1200 nmol/mL, [n.area] versus [S_{inj}] curves have negative curvatures. At the same time, the χ versus [S_{inj}] and $\bar{v}$ versus [S_{inj}] profiles are flat. Therefore, 1000–1200 nmol/mL is the point where the [S_0] $\gg$ [S] assumption begins to fail, because the amount of immobilized enzyme becomes a peptide cleavage rate controlling factor.

Thus, the diffusion limited nature of the immobilized trypsin digestion, column surface area, and immobilized trypsin load per surface area are the main limiting factors of the approximate linear response range of the IMER, i.e., lower and upper limits of quantification (LLOQ and ULOQ). But LLOQ and ULOQ can be influenced by detergent addition and adjustment of V_{inj} and F, as discussed below.

Effect of detergent type and concentration

The profiles of [n.area], χ and $\bar{v}$ versus detergent type and concentration can be rationalized with two possible effects of the detergent: (1) enhanced protein denaturing, which makes the peptide sequences more accessible to cleavage and accelerates peptide production; and (2) increased solubility of the peptide products in the mobile phase, facilitating their removal from the IMER.

Zwittergent 3–12 has a CMC of 2–4 mM (0.07–0.15%). The CMC of Invitrosol was unknown, being a proprietary detergent mix. Nevertheless, based on the effect of Zwittergent, the main difference in experiments 1/2 versus 3/4 was that the detergent concentration was approximately above versus under the CMC, respectively. This is most likely the reason that increasing the detergent concentration enhanced the LC–MS/MS signal intensities significantly only at <0.1% Zwittergent and <1× Invitrosol concentrations.

Therefore, the CMC of the detergent is an important consideration in selecting detergents and their concentration for enhancing IMER trypsin digestion.

Effect of mobile phase flow rate

The flow rate (F) has two main effects: (1) to determine the reaction time, $t_R = \frac{\mathrm{Vol_{col}}}{F}$ and (2) to determine the efficacy of product removal from the IMER, especially if the peptide product has some affinity to the particle surface leading to its accumulation at the partitioning boundary (Figure 1, dashed red line).

In general, increasing F had a negative effect on χ due to shorter t_R. However, increasing F seemed to have much less or no negative effect at higher $[S_{inj}]$ (Figure 3 versus 4). This is most likely because at higher $[S_{inj}]$, the negative effect of the reduced t_R is compensated by a positive effect, which is the more effective removal of the cleavage products. Therefore, in terms of application to protein quantification, increasing F results in less method sensitivity and a higher LLOQ, but it can also help to increase the ULOQ.

Effect of injection volume

The injection volume ($\mathrm{Vol_{inj}}$) can have two main effects: (1) larger $\mathrm{Vol_{inj}}$ increases the amount of protein passing through the IMER; therefore, the amount of peptides collected on the trapping column is also increased, enhancing LC–MS/MS signal intensity; and (2) if the protein has some affinity to the particle surface through ionic, H-bonding, and van der Waals interactions, increasing $\mathrm{Vol_{inj}}$ can cause accumulation of the protein at the partitioning boundary, despite the excess of trypsin in the pores (Figure 1, blue dashed line). Consequently, $[S_0]$ is no longer the sole cleavage rate determining factor.

Even at relatively low BSA concentrations <2 nmol/mL, the benefits of increasing $\mathrm{Vol_{inj}}$ above 100 μL reached its limit by all measures (Figures 4). At BSA concentrations >2 nmol/mL (especially at low F), increasing $\mathrm{Vol_{inj}}$ had a significantly negative effect on χ and $\bar{\nu}$ (Figure 3). Therefore, increasing $\mathrm{Vol_{inj}}$ results in better LC–MS/MS sensitivity only at low protein concentration and lowers the LLOQ, but at the same time, also lowers the ULOQ, overall leading to more narrow linear dynamic range.

Optimization

The JMP software also allowed the combination of each y-outcome, [n.area], $[P_{out}]$, χ, and $\bar{\nu}$ with individual weight functions (desirability) on a scale of 0–1 (shown in the Supporting Information). Taking advantage of this interactive software function of JMP, we selected the optimum value of the method variables in the following order and considerations. Zwittergent was chosen as detergent because overall it gave better LC–MS/MS sensitivity than Invitrosol. The optimal Zwittergent concentration range was at 0.15–0.2%, near the CMC of Zwittergent. The optimal range of F was 25–30 μL/min; with minimum negative effect on χ and $\bar{\nu}$. The optimal range of $\mathrm{Vol_{inj}}$ was 25–50 μL by maximizing LC–MS/MS signal intensity at low BSA concentrations while avoiding the saturation of the IMER at high BSA concentrations.

With the above method conditions, the linear quantification range for BSA in the injection solution was approximately 1–500 nmol/mL. As a test of the accuracy of the empirical model predictions, we performed an experiment where we set the flow rate at 25 μL/min, and injected 50 μL of BSA samples at <500 nmol/mL. As predicted, the optimal Zwittergent concentration that still gave improvement in LC–MS/MS dilution curve slopes was 0.2% Zwittergent concentration in the injection solution (Figure 5).

Conclusions

Optimization of immobilized trypsin digestion for quantitative LC–MS/MS analysis can be a very tedious and time-consuming task by trial-and-error approach. By applying the DoE approach for optimization, we gained insights into the physicochemical behavior of a trypsin IMER as well as finding the optimal conditions for analysis of our model protein. It is important to note that the optimal conditions in this work apply only to our specific trypsin column dimensions, detergents, digestion buffer composition, and protein concentration range. In this report, we examined the digestion of only one protein, and we did not examine biological matrix effects. However, we mention that we applied the optimal conditions found for BSA to the online trypsin digestion-coupled LC–MS/MS quantification of apolipoproteins in serum using a value assigned serum pool as the calibrator.[15] The dilution series of the calibrator pool and unknown sera were diluted 100-fold before analysis to adjust to the optimal protein concentration range found in this work. The resulting linear quantification range of the apolipoproteins was similar to that of BSA. We hope that the insights we shared here based on BSA will provide guidance to other users to more effectively optimize the quantitative analysis of proteins at applicable concentration ranges in biological matrices and take advantage of this powerful technology.

References

1. van den Broek I, Nouta J, Razavi M, Yip R, Bladergroen MR, Romijn FPHTM, Smit NPM, Drews O, Paape R, Suckau D, Deelder AM, van der Burgt YEM, Pearson TW, Anderson NL, Cobbaert CM. Quantification of Serum Apolipoproteins A-I and B-100 in Clinical Samples Using an Automated SISCAPA-MALDI-TOF-MS Workflow. Methods. 2015; 81: 74–85. [PubMed: 25766926]
2. Smit NPM, Romijn FPHTM, van den Broek I, Drijfhout JW, Haex M, van der Laarse A, van der Burgt YEM, Cobbaert CM. Metrological Traceability in Mass Spectrometry-based Targeted Protein Quantitation: A Proof-of-principle Study for Serum Apolipoproteins A-I and B100. J Proteomics. 2014; 109: 143–161. [PubMed: 24972322]
3. Switzar L, Giera M, Niessen WMA. Protein Digestion: An Overview of the Available Techniques and Recent Developments. J Proteome Res. 2013; 12: 1067–1077. [PubMed: 23368288]
4. Lassman ME, McLaughlin TM, Somers EP, Stefanni AC, Chen Z, Murphy BA, Bierilo KK, Flattery AM, Wong KK, Castro-Perez JM, Hubbard BK, Roddy TP. A Rapid Method for Cross-species Quantitation of Apolipoproteins A1, B48 and B100 in Plasma by Ultra-performance Liquid Chromatography/Tandem Mass Spectrometry. Rapid Commun Mass Spectrom. 2012; 26: 101–108. [PubMed: 22173797]
5. Hoofnagle AN, Becker JO, Oda MN, Cavigiolio G, Mayer P, Vaisar T. Multiple-reaction Monitoring-mass Spectrometric Assays Can Accurately Measure the Relative Protein Abundance in Complex Mixtures. Clin Chem. 2012; 58: 777–781. [PubMed: 22307200]
6. Agger SA, Marney LC, Hoofnagle AN. Simultaneous Quantification of Apolipoprotein A-I and Apolipoprotein B by Liquid-Chromatography–Multiple-reaction–Monitoring Mass Spectrometry. Clin Chem. 2010; 56: 1804–1813. [PubMed: 20923952]

7. Kay RG, Gregory B, Grace PB, Pleasance S. The Application of Ultra-performance Liquid Chromatography/Tandem Mass Spectrometry to the Detection and Quantitation of Apolipoproteins in Human Serum. Rapid Commun Mass Spectrom. 2007; 21: 2585–2593. [PubMed: 17639571]

8. Davidsson P, Hulthe J, Fagerberg B, Olsson BM, Hallberg C, Dahllof B, Camejo G. A Proteomic Study of the Apolipoproteins in LDL Subclasses in Patients with the Metabolic Syndrome and Type 2 Diabetes. J Lipid Res. 2005; 46: 1999–2006. [PubMed: 15995172]

9. Van Den Broek I, Romijn FPHTM, Smit NPM, Van Der Laarse A, Drijfhout JW, Van Der Burgt YEM, Cobbaert CM. Quantifying Protein Measurands by Peptide Measurements: Where Do Errors Arise? J Proteome Res. 2015; 14: 928–942. [PubMed: 25494833]

10. Regnier FE, Kim JH. Accelerating Trypsin Digestion: The Immobilized Enzyme Reactor. Bioanalysis. 2014; 6: 2685–2698. [PubMed: 25411709]

11. Kim JH, Inerowicz D, Hedrick V, Regnier F. Integrated Sample Preparation Methodology for Proteomics: Analysis of Native Proteins. Anal Chem. 2013; 85: 8039–8045. [PubMed: 23937592]

12. Nicoli R, Rudaz S, Stella C, Veuthey JL. Trypsin Immobilization on an Ethylenediamine-based Monolithic Minidisk for Rapid On-line Peptide Mass Fingerprinting Studies. J Chromatogr A. 2009; 1216: 2695–2699. [PubMed: 18962647]

13. Lim LW, Tomatsu M, Takeuchi T. Development of an On-line Immobilized-enzyme Reversed-phase HPLC Method for Protein Digestion and Peptide Separation. Anal Bioanal Chem. 2006; 386: 614–620. [PubMed: 16724223]

14. Moore S, Hess S, Jorgenson J. Characterization of an Immobilized Enzyme Reactor for On-line Protein Digestion. J Chromatogr A. 2016; 1476: 1–8. [PubMed: 27876348]

15. Toth CA, Kuklenyik Z, Jones JI, Parks BA, Gardner MS, Schieltz DM, Rees JC, Andrews ML, McWilliams LG, Pirkle JL, Barr JR. On-column Trypsin Digestion Coupled with LC–MS/MS for Quantification of Apolipoproteins. J Proteomics. 2017; 150: 258–267. [PubMed: 27667389]

16. Chaplin, M, Bucke, C. Enzyme Technology. Vol. Chapter 3. Cambridge University Press; Cambridge, UK: 1990. The Preparation and Kinetics of Immobilsed Enzymes; 80–100.

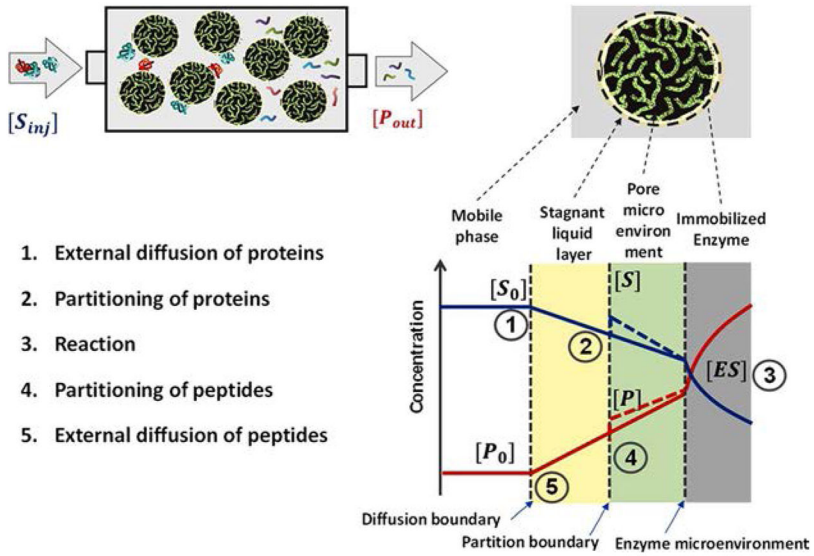

Figure 1.

Schematic showing the concentration gradients of proteins and peptide cleavage products produced around a porous particle with immobilized trypsin. [S_{inj}], [S_0], and [S] are the concentration of the protein substrate in the injection plug, at the diffusion boundary and at the partition boundary, respectively. [P], [P_0], and [P_{out}] are the concentrations of the peptide product at the partition boundary, at the diffusion boundary and in the injection plug leaving the IMER, respectively. [ES] is the concentration of immobilized enzyme/protein complex inside the pore. The continuous blue line represents the concentration gradient of the protein (substrate, S). The dashed blue line represents the concentration gradient of the protein if partitioning on the particle surface occurs. The red line represents the concentration gradient of the peptide (product, P). The dashed red line represents the concentration gradient of the peptide if partitioning on the particle surface occurs. *Note*: IMER, immobilized enzyme reactor.

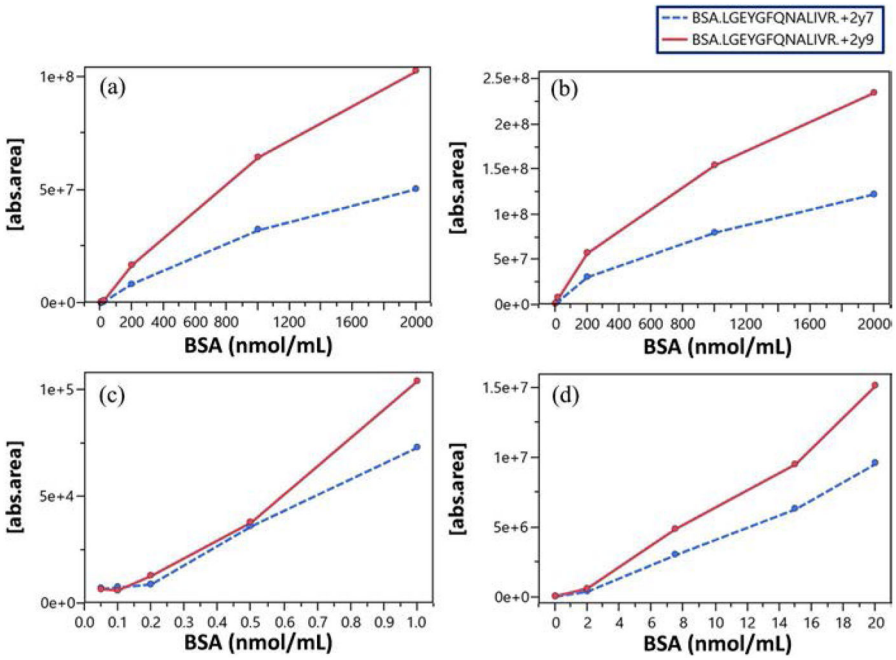

Figure 2.

Representative experimental peak area versus BSA concentration profiles at 100 μL injection volume and 25 μL/min flow rate using Invitrosol (a and c) and Zwittergent (b and d) as detergent. BSA concentrations: a and b, 2–2000 nmol/mL; c, 0.05–1 nmol/mL; and d, 0.02–20 nmol/mL. *Note*: BSA, bovine serum albumin.

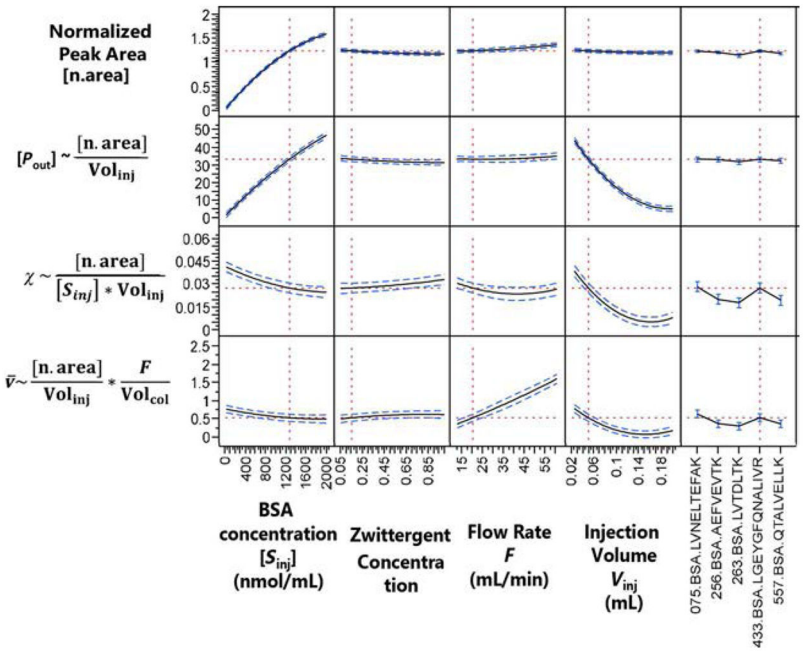

Figure 3.

Response surface prediction profiles based on Experiment 2 in Table 1, using BSA (2–2000 nmol/mL) and Zwittergent detergent (0.05–1%). [n.area]: normalized LC–MS/MS peak areas (R^2 = 0.92); [P_{inj}]: peptide concentration in the injection plug leaving the IMER (R^2 = 0.87), χ: digestion efficacy (R^2 = 0.29), and $\bar{v}$: digestion rate (R^2 = 0.30). *Note*: BSA, bovine serum albumin.

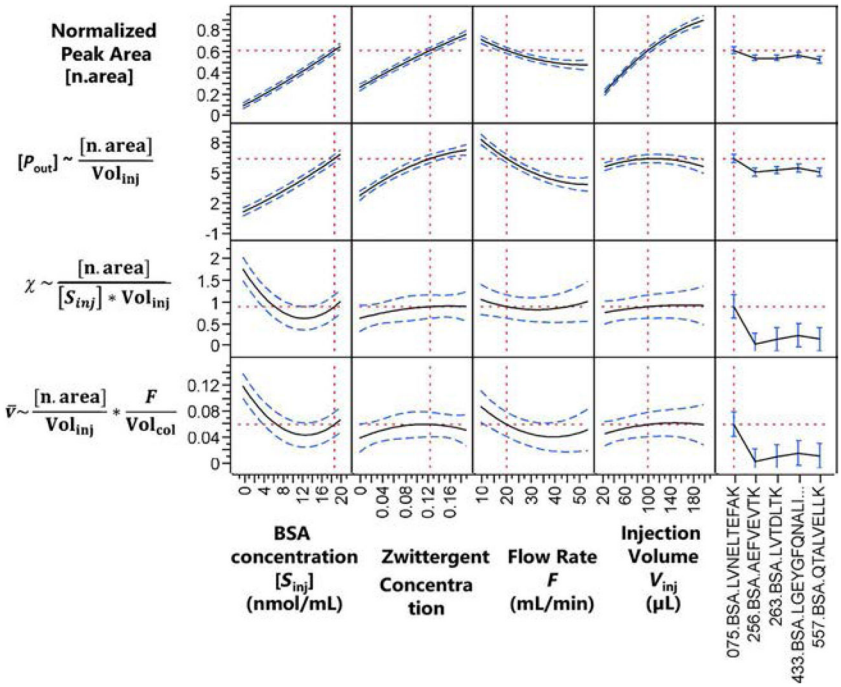

Figure 4.

Response surface prediction profiles based on experiment 4 in Table 1, using BSA (0.02–20 nmol/mL) and Zwittergent detergent (0.01–0.2%). [n.area]: normalized LC–MS/MS peak areas; (R^2 = 0.90); [P_{inj}]: peptide concentration in the injection plug leaving the IMER (R^2 = 0.77); χ: digestion efficacy (R^2 = 0.32); and $\bar{v}$: digestion rate (R^2 = 0.32). *Note*: BSA, bovine serum albumin; IMER, immobilized enzyme reactor.

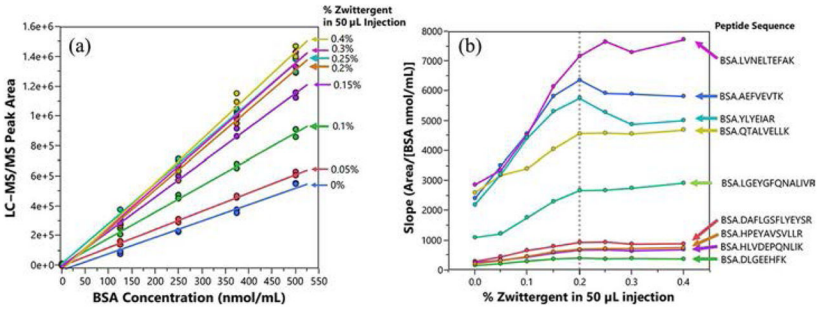

Figure 5.

Bovine serum albumin (BSA) dilution curves of a representative peptide (BSA. LGEYGFQNAIVR) at 0–0.4% Zwittergent 3–12 concentration in 50 µL injection volume and at 25 µL/min digestion buffer flow rate. (a) LC–MS/MS peak areas versus BSA concentration curves. (b) Dilution curve slopes versus Zwittergent concentration profiles for nine BSA peptides.

Table 1

Method parameters used in the four experiments. The concentration of the Invitrosol solution expressed with folds of dilution as prepared from 5× proprietary concentrate as purchased.

Experiment	Detergent	BSA concentration (nmol/mL)	Detergent concentration	Flow rate (μL/min)	Injection volume (μL)
1	Invitrosol	2, 20, 200, 1000, 2000	0.25×, 1×, 2.5×	12.5, 20, 60.5	25, 112.5, 200
2	Zwittergent	2, 20, 200, 1000, 2000	0.01, 0.5. 1.0%	12.5, 20, 60.5	25, 112.5, 200
3	Invit rosol	0.05, 0.1, 0.2, 0.5, 1	0.05×, 0.2×, 0.5×, 1×	12.5, 15, 26.5, 60.5	25, 50, 100, 200
4	Zwittergent	0.2, 2, 7.5, 15, 20	0.01, 0.04, 0.1. 0.2	12.5, 15, 26.5, 60.5	25, 50, 100, 200

BSA, bovine serum albumin.